Radiative and Non-radiative Processes in Intermediate Band Solar Cells

Stanko Tomić
Joule Physics Laboratory, School of Computing, Science and Engineering, University of Salford, UK

***Abstract*—Intermediate band solar cells (IBSC) have emerged as an alternative design for third generation solar cells that could lead to dramatical improvements of the power conversion efficiencies. For this concept to work the intermediate band (IB) has to be located in the forbidden energy gap of the barrier material and to be separated by zero density of states from the valence and conduction band of the barrier material. We have demonstrated that a $\mathrm{k}\cdot\mathrm{p}$ multiband theory with periodic boundary conditions can easily be applied to predict electronic and absorption characteristics, as well as radiative and non-radiative carrier life-times between IB induced by semiconductor quantum dot (QD) arrays. We have identified that the most detrimental effect that might affect proper operation of the IBSC is caused by very fast, ∼ps, Auger electron cooling non-radiative process. We discuss possible QD array designs that can suppress fast Auger electron cooling.**

I. Introduction

The intermediate band solar cell (IBSC) has been proposed as a means to improve efficiency over that of a single gap solar cell. [1], [2] The IBSC comprises the so called "intermediate band material", having an electronic band (intermediate band, IB) inside what otherwise would be a conventional semiconductor bandgap, E_G. We will denote the total bandgap of the semiconductor as E_G, and its two parts, measured from the centre of the IB, as E_L and E_H. To achieve its higher efficiency potential, the IB allows absorption of below-bandgap energy photons on transitions from the valence band (VB) to the IB and from the IB to the conduction band (CB). These absorption processes induce the corresponding carrier generation rates, and these add up to the conventional carrier generation from the VB to the CB. Once carriers have been generated, they can also recombine. For preserving the output voltage of the cell (equal to the difference of electron and hole quasi-Fermi levels, $eV = E_{FC} - E_{FV}$, where e the electron charge), [3] it is necessary that quasi-Fermi level separation exists between the CB quasi-Fermi level (E_{FC}) and the IB quasi-Fermi level (E_{FI}), and also between the VB quasi-Fermi level (E_{FV}) and E_{FI}. These are increasingly difficult to achieve as the recombination rates between IB and CB and between IB and VB, involving processes other than radiative recombination, increases too.

II. Theoretical method

To solve the multi-band system of Schrödinger equations, the **k·p** equation, for the semiconductor quantum dots (QD) array, the plane wave (PW) methodology is employed as an expansion method. [4], [5] In the PW representation the eigenvalues (E_n) and coefficients ($A_{n,\mathbf{k}}$) of the n^{th}-eigenvector, $[\psi_n(\mathbf{r}) = \sum_{\mathbf{k}} A_{n,\mathbf{k}} e^{i\mathbf{kr}}]$, are linked by the relation

$$\sum_{m,\mathbf{k}'} h_{m,n}(\mathbf{k}',\mathbf{k}) A_{n,\mathbf{k}} = E_n \sum_{\mathbf{k}} A_{n,\mathbf{k}} \tag{1}$$

where $h_{m,n}(\mathbf{k}',\mathbf{k})$ are the Fourier transform of the Hamiltonian matrix elements, and $m,n \in \{1,...,8\}$ are the band indexes of the 8-band **k·p** Hamiltonian. All the elements in the Hamiltonian matrix, Eq. (1), can be expressed as a linear combination of different kinetic and strain related terms and its convolution with the characteristic function of the actual QD shape, $\chi_{\mathrm{qd}}(\mathbf{k})$. [6], [5]

The PW based **k·p** method inherently assumes *periodic Born-von Karman boundary conditions* and is particularly suited for analysis of the QD array structures. The electronic structure of such an array is characterized by a Brillouin zone (BZ) determined by the QD array dimensions. [7], [8], [9] To calculate the electronic structure the only modification to the basis set is to replace the reciprocal lattice vectors in the PW expansion with those shifted due to the QD-superlattice (QD-SL):

$$k_\nu \rightarrow k_\nu + K_\nu \tag{2}$$

where $0 \leq K_\nu \leq \pi/L_\nu$, and the L_ν are the super-lattice vectors in the $\nu = (x,y,z)$ directions. This allows sampling along the $\mathbf{K}$ points of a QD-SL Brillouin zone to be done at several points at the cost of the single QD calculation at each point $\mathbf{K}$, avoiding laborious calculations of the large QD clusters. The QD array wave functions throughout the QD Brillouin zone become $\Psi_{n,\mathbf{K}}(\mathbf{r}) = \sum_{\mathbf{k}} A_{n,\mathbf{K}} e^{i(\mathbf{k}+\mathbf{K})\mathbf{r}}$. All the results presented here were obtained by using the kppw code. [4], [5]

III. Model QD array

The model QD arrays considered here consist of InAs/GaAs QDs with truncated pyramidal shape, Fig. 1. The size and shape of the QD is controlled by the pyramid base length, b, its height h, and truncation factor, t, defined as a ratio between length of the pyramid side at h, and length of the pyramid base b. The QDs are embedded in the tetragonal-like unit cell. The vertical periodicity of the QD array is controlled by $L_z = d_z + h + L_{WL}$, where d_z is the vertical separation of the QDs in subsequent layers.

978-1-4673-1604-0/12/$31.00 ©2012 IEEE

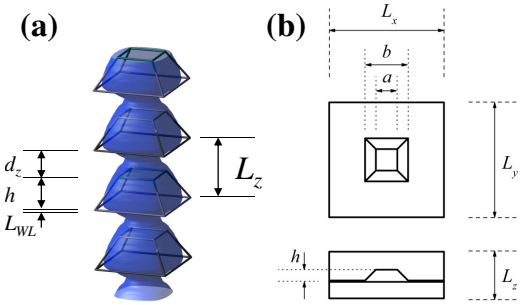

Fig. 1: Schematic of the model QD array (a), and QDs that makes array (b). QD truncation factor is defined as $t = a/b$, while all the other relevant parameters are defined in the main text

IV. Results and Discussion

For typical QD array, made of truncated pyramidal InAs/GaAs QDs with $b = 10$ nm, $h = 2.5$ nm, and $t = 0.5$, and with vertical spacing between the dots in the array of $d_z = 5$ nm, we have estimated energy gaps between valence band (VB) and intermediate band (IB) of 1.2 eV and between IB and conduction band (CB) of 0.124 eV. By varying the QD sizes keeping periodicity in the z direction constant, our predictions suggest that the most promising design for an IB material that will exhibit its own quasi-Fermi level is to employ small InAs/GaAs QDs (6-10 nm QD lateral size) [8]. With appropriate design of the QD array structural parameters: (1) it is possible to achieve the regions of pure zero DOS between IB and the rest of the CB states, that is desirable for photon sorting and increased efficiency of device, and (2) it is possible to achieve the strong optically allowed excitation between IB and CB [10], [11]. Analysis of various radiative and nonradiative times, Table I, indicates that: (i) the ratio between CB to IB and IB to VB radiative times is 50, (ii) although phonon related relaxation time between CB and IB (56 ns) amounts to a half of the radiative relaxation time between CB and IB (109 ns), it is still one order of magnitude larger than the IB to VB radiative time (2.1 ns), (ii) non-radiative phonon absorption process that promotes electrons from IB to CB is very slow (650 ns) and probably would not significantly affect the transport properties of the IBSC, (iv) nonradiative Auger bi-exciton relaxation, Fig. 2, time (8.4 ns) is longer then radiative IB to VB relaxation time, indicating that this process will still be predominately radiative, (v) most detrimental effect on transport properties can originate from non- radiative Auger electron cooling process (2 ps), Fig. 2, that is three orders of magnitude faster that any other relaxation process in the IBSC [10], [11]. Special attention needs to be paid in the design of the IBSC structures in order to suppress the effects of electron cooling and to provide an increased efficiency of the IBSCs. We have shown recently that with appropriate band structure engineering, it is possible

TABLE I: Radiative, LO phonon emission/absorption, and Auger scattering times of InAs/GaAs QD array IBSC considered in the main text.

Type	minibands	Radiative (ns)	Phonons [e/a] (ns)	Auger (ns)
CB→IB	$e1 \rightarrow e0$	109	56/650	2×10^{-3}
IB→VB	$e0 \rightarrow h0$	2.1		8.4

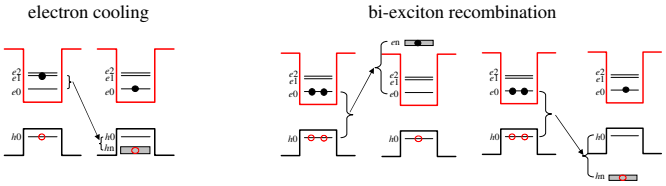

Fig. 2: Illustration of two different Auger processes: electron cooling (left) and bi-exciton recombination (right).

to place the intraband Auger electron cooling decay timescale in the ns range [12]. Such an optimised design requires a VB confinementless QD structure or Sb containing alloys in the barrier region in order to induce the type-II alignment and spatial electron/hole separation [10].

Predicted efficiency of IBSC in which nonradiative processes are suppressed and operation is dominated by radiative processes only, based on drift-diffusion model [13], and using realistic parameters obtained above, is 39% under maximal sun concentration [11]. This is increase of 56% compared to simple QD solar cell.

Our work provides a very important conceptual message – with appropriate treatment of relevant radiative and nonradiative effects, the multiband envelope function Hamiltonians with periodic boundary conditions are fully capable of capturing the all relevant effects determining operation of the QD based intermediate band solar cells.

References

[1] A. Luque and A. Martí, "Increasing the efficiency of ideal solar cells by photon induced transitions at intermediate levels," *Phys. Rev. Lett.*, vol. 78, no. 26, pp. 5014–5017, Jun 1997.

[2] A. Luque and A. Marti, "The intermediate band solar cell: Progress toward the realization of an attractive concept," *Advanced Materials*, vol. 22, pp. 160–174, 2010.

[3] ——, "A metallic intermediate band high efficiency solar cell," *Prog. Photovoltaics*, vol. 9, no. 2, pp. 73–86, MAR-APR 2001.

[4] S. Tomić, A. G. Sunderland, and I. J. Bush, "Parallel multi-band $k \cdot p$ code for electronic structure of zinc blend semiconductor quantum dots," *J. Mater. Chem.*, vol. 16, pp. 1963–1972, 2006.

[5] N. Vukmirović and S. Tomić, "Plane wave methodology for single quantum dot electronic structure calculations," *J. Appl. Phys.*, vol. 103, no. 10, p. 103718, 2008.

[6] A. D. Andreev, J. R. Downes, D. A. Faux, and E. P. O'Reilly, "Strain distributions in quantum dots of arbitrary shape," *J. Appl. Phys.*, vol. 86, pp. 297–305, 1999.

[7] O. L. Lazarenkova and A. A. Balandin, "Miniband formation in a quantum dot crystal," *Journal of Applied Physics*, vol. 89, no. 10, pp. 5509–5515, 2001.

[8] S. Tomić, T. S. Jones, and N. M. Harrison, "Absorption characteristics of a quantum dot array induced intermediate band: Implications for solar cell design," *Appl. Phys. Lett.*, vol. 93, no. 26, p. 263105, 2008.

[9] J. W. Klos and M. Krawczyk, "Two-dimensional gaas/algaas superlattice structures for solar cell applications: Ultimate efficiency estimation," *Journal of Applied Physics*, vol. 106, no. 9, p. 093703, 2009.

[10] S. Tomić, "Intermediate-band solar cells: Influence of band formation on dynamical processes in inas/gaas quantum dot arrays," *Phys. Rev. B*, vol. 82, p. 195321, Nov 2010.

[11] S. Tomić, *in Next Generation of Photovoltaics*. (Springer, Heidleberg 2012).

[12] S. Tomić, A. Martí, E. Antolín, and A. Luque, "On inhibiting auger intraband relaxation in inas/gaas quantum dot intermediate band solar cells," *Applied Physics Letters*, vol. 99, no. 5, p. 053504, 2011.

[13] R. Strandberg and T. W. Reenaas, "Photofilling of intermediate bands," *Journal of Applied Physics*, vol. 105, no. 12, p. 124512, 2009.